Carbohydrate Polymers 149 (2016) 175–185

Contents lists available at ScienceDirect

Carbohydrate Polymers

journal homepage: www.elsevier.com/locate/carbpol

Novel cross linked guar gum-*g*-poly(acrylate) porous superabsorbent hydrogels: Characterization and swelling behaviour in different environments

KSV Poorna Chandrika[b], Anupama Singh[a,*], Abhishek Rathore[c], Anil Kumar[d]

[a] Division of Agricultural Chemicals, ICAR-Indian Agricultural Research Institute, New Delhi 110012, India
[b] Division of Agricultural Chemicals, ICAR-Indian Institute of Oilseeds Research, Rajendernagar, Hyderabad, Telangana 500030, India
[c] Biometrics, CEG, International Crops Research Institute for the Semi-arid tropics, Patancheru 502324, India
[d] Division of Design of Experiments, ICAR-Indian Agricultural Statistics Research Institute, New Delhi 110012, India

ARTICLE INFO

Article history:
Received 17 December 2015
Received in revised form 15 April 2016
Accepted 18 April 2016
Available online 21 April 2016

Keywords:
Guar gum
Porous
Swelling
Crosslinking
Hydrogels

ABSTRACT

A new series of eco-friendly cross linked guar gum-*g*-poly(acrylate) porous superabsorbent hydrogels was prepared by *in situ* grafting polymerization and cross-linking on to a natural guar gum employing *N*,*N*-methylene bis acrylamide as cross linker. Morphological and structural characterization of the prepared hydrogels (SPHs) done by Fourier-transform infrared spectroscopy (FTIR), scanning electron microscopy (SEM) and solid state C^{13} NMR spectroscopy confirmed formation of porous grafted and crosslinked hydrogel structure. Increase in cross linker concentration in the feed mass exhibited decrease in porosity and increase in density of the hydrogels. Swelling of an optimized hydrogel (SPH) in response to external stimuli namely, salt solutions, fertilizer solutions, temperature, and pH exhibited high swelling ratios in various environments. Swelling rate of the SPH was faster than the corresponding nonporous superabsorbent hydrogel. The prepared hydrogels can serve as excellent carriers of pesticides, fertilizers and agriculturally important microbes. Biocontrol formulations based on a representative SPH exhibited excellent shelf-life characteristics and bioefficacy against phytopathogenic fungus *Pythium aphanidermatum*.

1. Introduction

Superabsorbent hydrogels are cross-linked hydrophilic polymers with three dimensional network structures consisting of acidic, basic, or neutral monomers which are able to imbibe large amounts of water and other fluids (Omidian & Park, 2002). Because of their network structures and the possibility of rearrangements of hydrophobic/hydrophilic domains during the swelling process, including entanglements and crystalline regions, these polymers are water insoluble (Choi et al., 2007). Versatile fluid retention-release character qualifies superabsorbent hydrogels as smart devices in many fields such as agriculture (Puoci, Iemma, & Spizzirri, 2008), hygienic products (Kosemund et al., 2009), waste water treatment (Kasgoz & Durmus, 2008) and drug-delivery (Wang, Zhang, & Wang, 2009). The swelling properties of hydrogels are mainly related to the elasticity of the network, the extent of cross-linking, and porosity of the polymer (Kim and Park, 2004). These properties also play an important role in controlled release formulations based on hydrogels.

Among the new generation hydrogels, super porous hydrogels are lightly crosslinked hydrophilic polymers that can absorb aqueous solutions upto hundreds of times their own weight in shorter duration (Hyojin, Kinam, & Dukjoon, 2006). The fast swelling of these polymers can be related to capillary wetting of interconnected open pores (Yin, Fei, Cui, Tang, & Yin, 2007). Of late, biopolymeric super porous hydrogels are of interest due to their multifarious applications in domains such as drug delivery and tissue engineering *etc.* (Chen, Park, & Park, 1999). Because of their biocompatibility, biodegradability and non-toxicity, polysaccharides and protein-based porous hydrogels have created extensive interest (Omidian, Rocca, & Park, 2006). Guar gum, a non-ionic galactomannan polysaccharide seed gum derived from *Cymaposis tetragonolobus*, bears linear chain β-D-mannopyranose joined by (1–4) linking with α-D-galactopyranosyl units (Sinha & Kumria, 2001) attached by 1, 6 links in ratio of 1:2. Because of the immense potential and low price, this versatile polymer is used as a vehicle in

* Corresponding author.
E-mail address: anupama.chikara@gmail.com (A. Singh).

http://dx.doi.org/10.1016/j.carbpol.2016.04.077
0144-8617/

controlled release applications (Guo, Skinner, Harcum, & Barnum, 1998). However like other polysaccharides, guar gum is highly susceptible to microbial attack. Chemical modification such as grafting inhibits fast microbial degradation and also improves the swelling and flocculation properties of guar gum (Zhang, Li, & Wang, 2006). Use of guar gum as backbone to prepare porous hydrogels in *hitherto* unknown. In the present article, novel user friendly open air synthesis of crosslinked guar gum-*g*-poly(acrylate) porous superabsorbent hydrogels has been reported. In most of available reports, extensive investigations on effect of reaction parameters on swelling behaviour are lacking for porous hydrogels. The effects of various reaction parameters namely cross linker concentrations, initiator concentration, volume of water per unit feed, nature of foam stabilizers and foaming aids and their concentrations, duration of reaction *etc*. has been presented in detail and supported by structure characterisation. Effect of sequence of addition of reactants in the feed mass is also discussed. In the second part of the study, swelling behaviour of an optimized SPH as a function of external stimuli namely, pH, salts and fertilizers and water quality has been reported.

2. Materials and methods

2.1. Materials

Commercial guar gum (purity 95%), acrylamide, *N*,*N*′-methylenebisacrylamide, *N*,*N*,*N*′,*N*′ tetramethylenediamine (TEMED) and sodium bicarbonate were purchased from SD Fine (Pvt) Ltd., Mumbai, India. Persulphate initiator, surfactants (FS1, sodium dodecyl sulphate; FS 2, AC-DI-SOL; FS 3, sodium lauryl ether sulphate; FS 4, ammonium lauryl sulphate) and foaming aids (oxalic acid, citric acid and acetic acid) were purchased from Merck, (Pvt) Ltd. Mumbai, India. All the reagents were used as such without further purification.

2.2. Synthesis of porous cl-GG-g-poly(acrylate) hydrogels

The hydrogels were prepared by free radical grafting polymerization technique employing persulphate-TEMED redox initiator system. A general method of preparation followed in earlier reports (Chen et al., 1999; Guo and Gao, 2007; Park, Shalaby, & Park, 1993), involves sequential addition of monomer, cross linker, initiator, foam stabilizer and the foaming aid in distilled water under inert atmosphere at 70–80 °C. In the present study, six different sequences of addition of reactants were tried (Table 2). A typical procedure comprised dissolution of all the reagents including the backbone in distilled water. pH was adjusted to 5–5.5 (slightly acidic) and the reaction was initiated at 50 °C by the persulphate-TEMED redox pair. The time for harmonizing gelation and foaming reactions was standardised. The solution was kept undisturbed for a specific period. The resultant gel were washed, dehydrated and dried in hot air oven. Details of reactant levels investigated during standardization are depicted in Table 1.

The hydrogels were characterized by FT-IR spectra recorded in KBr disc on a Bruker Fourier Transform Infrared Spectrophotometer under dry air at room temperature. Solid state C^{13} NMR spectra of optimized SPH was recorded on a BRUKER DSX 300 instrument operating at 7.04 T, carbon frequency 75.47 MHz for carbon. Crosslinker and monomer were characterized by liquid state C^{13} NMR using BRUKER Avance instrument. Scanning electron microscopy images were obtained with a Zeiss EVO series scanning electron microscope (EVO 50) with resolution of 2.0 nm at 30 kV. Elemental analysis (CHNS analyser) of SPH were recorded in Varian micro cube elementar, Germany operating at combustion furnace temperature 1150 °C, reduction furnace temperature 850 °C and gas flow (Helium) 200 ml/min with an accuracy of ±0.01%(abs).

2.3. Water absorbency measurements

A sample weighing 0.1 g (particle size 100–240 mesh size) was immersed in the excess of distilled water (pH 7.0, EC 0.001 mhos/cm) in triplicate and kept at 50 °C till equilibration. Free water was filtered through a nylon sieve (200 mesh size), gel allowed to drain on sieve for 10 min, and finally weighed. The water absorbency (Q_{H_2O}) was calculated using the following equation:

$$Q_{H_2O}\left(g/g\right) = w_2 - w_1/w_1$$

where w_1 is the weight of xerogel (dry hydrogel) and w_2 is the weight of equilibrated swollen gel. Q_{H_2O} was calculated as grams of water per gram of dry sample. The SPH exhibiting maximum absorption in distilled water was further evaluated in different salt solutions.

2.4. Salt solution absorbency measurements

SPH was milled to achieve particle size of the range 100–240 mesh size. Aqueous solutions of different strengths (5, 10, 15, and 20 mM) of four salts namely ammonium sulphate (AS), ammonium nitrate (AN), potassium nitrate (PN), sodium chloride (SC), and fertilizer namely urea (U) were prepared and used. The dried and milled sample was immersed in salt solution of a particular strength at 50 °C. The swollen gel was weighed after 24 h, using same equation as above. Similar experiment was repeated in tap water (pH 7.87, EC 1.099 mhos/cm), hard water, and aqueous solutions of pH 4, 7, and 9. Hard waters of three different strengths were prepared in the laboratory according to CIPAC standard method (Daasch, 1947) and labelled as hard water A (hardness 20 ppm, pH 5–6, and Ca:Mg ratio 50:50), hard water B (hardness 20 ppm, pH 8–9, and Ca:Mg ratio 80:20), and hard water C (hardness 500 ppm, pH 7–8, and Ca:Mg ratio 80:20).

2.5. Density and porosity measurements

For density measurement, the solvent replacement method was used (Tang, Yin, Pei, Zhang, & Wu, 2005). A piece of dried SPHC was taken and weighed. It was immersed in a predetermined volume of hexane in a graduated cylinder and the increase in hexane in a graduated cylinder and the increase in hexane volume was measured as the volume of the polymer. The density was calculated from the following equation:

$$Density = M_{SPH}/V_{SPH}$$

where, V_{SPH} is the volume of solvent displaced by SPH and M_{SPH} is the mass of the SPH. Experiment was done in triplicate. For porosity measurement, dried SPHs were immersed in hexane overnight and weighed after the excess hexane on the surface was blotted. The porosity was calculated from the equation (Chavda & Patel, 2009):

$$Porosity = V_P/V_T$$

where, $V_P = (V_T - V_{SPH})$ is the pore volume of SPH and V_T is the total volume of the SPH. Total volume of SPH was measured from its dimensions, as it was cylindrical in shape.

2.6. Shelf life and bioefficacy (in vitro) evaluation of SPH microbial formulations

To assess the suitability of porous hydrogels as carriers of microbes, a representative SPH hydrogel was employed to

Table 1
Levels of process parameters* standardised in preparation of GG-SPH.

Paramater	Levels/Types
[a]Method of preparation	4 (I, II, II, IV,V,VI)
[b]Cross linker concentration (wt% feed mass basis)	5 (0.01, 0.03, 0.1, 0.3, 0.7)
[c]Foam stabilizer type	4 (FS-1, FS-2, FS-3, FS-4)
[d]Foam stabilizer concentration (wt% feed mass basis)	5 (0.0, 0.3, 1.8, 3.6, 7.3)
[e]Water volume (ml/g feed mass)	5 (1.98, 3.96, 5.95, 7.93, 9.92)
[f]Foaming aid type	3 (OA-1, OA-2, OA-3)
[g]Porogen concentration (wt% feed mass basis)	7 (0.1–0.5, 0.7–1.2, 1.4–2.2, 2.3–2.9, 3.1–4.4, 4.8–6.6, 6.9–9.1)
[h]Backbone:Monomer Ratio	4 (0.7, 0.3, 0.2, 0.1)

[a] Synthesis parameters: weight ratio of monomer, cross linker, initiator, foam stabilizer, porogen to backbone: 1.5:1, 0.01:1, 0.05:1, 0.1:1 and 0.1:1, respectively, V_{H_2O} 5.95 ml/g feed.
[b] Synthesis parameters: weight ratio of monomer, initiator, foam stabilizer, porogen to backbone: 1.5:1, 0.05:1, 0.1:1 and 0.1:1, respectively, V_{H_2O} 5.95 ml/g feed.
[c] Synthesis parameters: weight ratio of monomer, cross linker, initiator, foam stabilizer, porogen to backbone: 1.5:1, 0.01:1, 0.05:1, 0.1:1 and 0.1:1, respectively, V_{H_2O} 5.95 ml/g feed.
[d] Synthesis parameters: weight ratio of monomer, cross linker, initiator, porogen to backbone: 1.5:1, 0.01:1, 0.05:1 and 0.1:1, respectively, V_{H_2O} 5.95 ml/g feed.
[e] Synthesis parameters: weight ratio of monomer, cross linker, initiator, foam stabilizer, porogen to backbone: 1.5:1, 0.01:1, 0.05:1, 0.1:1 and 0.1:1, respectively.
[f] Synthesis parameters: weight ratio of monomer, cross linker, initiator, foam stabilizer, porogen to backbone: 1.5:1, 0.01:1, 0.05:1, 0.1:1 and 0.1:1, respectively, V_{H_2O} 5.95 ml/g feed.
[g] Synthesis parameters: weight ratio of monomer, cross linker, initiator and foam stabilizer to backbone: 1.5:1, 0.01:1, 0.05:1 and 0.1:1, respectively, V_{H_2O} 5.95 ml/g feed.
[h] Synthesis parameters: weight ratio of monomer, cross linker, initiator, foam stabilizer and porogen tobackbone:1.5:1, 0.01:1, 0.05:1, 0.1:1 and 0.1:1, respectively, V_{H_2O} 5.95 ml/g feed.
* Superscript in left side column indicates sequence of standardization of process parameters. Sequential design was used.

Table 2
Outline of various process protocols employed for GG-SPH synyhesis.

Method I	Method II	Method III	Method IV	Method V	Method VI
Acrylamide + MBA in water	Acrylamide + MBA in water	Acrylamide + MBA in water	Acrylamide + MBA in water	Acrylamide + MBA in water	Acrylamide + MBA in water
↓	↓	↓	↓	↓	↓
Organic acid	Organic acid	Organic acid	Organic acid	Organic acid	Organic acid
↓	↓	↓	↓	↓	↓
TEMED	Foam stabiliser	TEMED	TEMED	Foam stabiliser	TEMED
↓	↓	↓	↓	↓	↓
Foam stabiliser+ Guar gum + APS	TEMED	Guar gum + APS	Foam stabiliser+ Guar gum + APS	TEMED	Guar gum + APS
↓	↓	↓	↓	↓	↓
Porogen	Guar gum + APS	Porogen	Porogen	Guar gum + APS	Porogen
↓	↓	↓	↓	↓	↓
Heat at 50 °C for 10-15 min	Porogen	Heat at 50 °C for 10-15 min	Heat at 50 °C for 4 hrs	Porogen	Heat at 50 °C for 4 hrs
	↓			↓	
	Heat at 50 °C for 10-15 min			Heat at 50 °C for 4 hrs	

develop formulations containing *Trichoderma harzianum (Thz)* and *Pseudomonas fluorescens (Pflo)* immobilized individually into the hydrogel matrix. Dry formulations were prepared (moisture 0–5%) and care was taken to immobilize 10^8–10^{11} c.f.u. (colony forming units) of *Thz* and *Pflo* per gram carrier in all the compositions. Formulations (DSPH-*Thz* and DSPH-*Pflo*) were stored at test temperatures 25 °C, in BOD incubators along with control (*Thz* and *Pflo*).

Sampling from the compositions and the absolute controls of *Thz* or *Pflo* was done periodically at intervals of 0, 15, 30, 60, 90, 120, 150 and 180 days by dilution plate technique. Percent viability in terms of log cfus per gram formulation was calculated. The term CFU here refers to colony forming units in case of *T. harzianum* and cell forming units in case of *P. fluorescens*.

All the compositions and controls were evaluated periodically (0, 15, 30, 60, 90, 120, 150 and 180 d) for their bioefficacy against *Pythium aphanidermatum* (*in vitro*). Formulation (0.1 g) from each treatment was uniformly dispersed in the growth medium in Petri plate and incubated in a B.O.D. incubator at 28 °C. Each treatment was replicated thrice. After 5–7 days, at full growth stage of pathogen, percent inhibition of pathogen was calculated as:

$$I = \frac{C - T}{C} \times 100$$

where, C = pathogen colony diameter in control and T = pathogen colony diameter in bioagent treated plates.

2.7. Statistical analysis

The experiments on effect of various parameters on water absorbency values were conducted using completely randomized design. To identify the best treatment combinations, the data were analysed by one-way classified analysis using PROC GLM procedure of SAS package (SAS Institute, Cary, NC).

3. Results and discussion

3.1. Characterisation of porous hydrogel (SPH)

3.1.1. FT-IR of guar gum, and grafted porous hydrogel

The FT-IR spectra of native guar gum, acrylamide and *cl*-gg-*g*-poly(acrylate) (SPH) are shown in Fig. 1. The absorption bands of guar gum (GG) at 1661 cm^{-1} assigned to H—OH bending and at 1439 cm^{-1} assigned to C—OH bending vibration almost disappeared in FTIR of SPH (Fig. 1), where new bands at 1665 cm^{-1} (C=O stretching of COOH groups), 1435 cm^{-1} (O—H bending) and ≈1300 cm^{-1} (C—O stretching of carboxylic acid group) appeared.

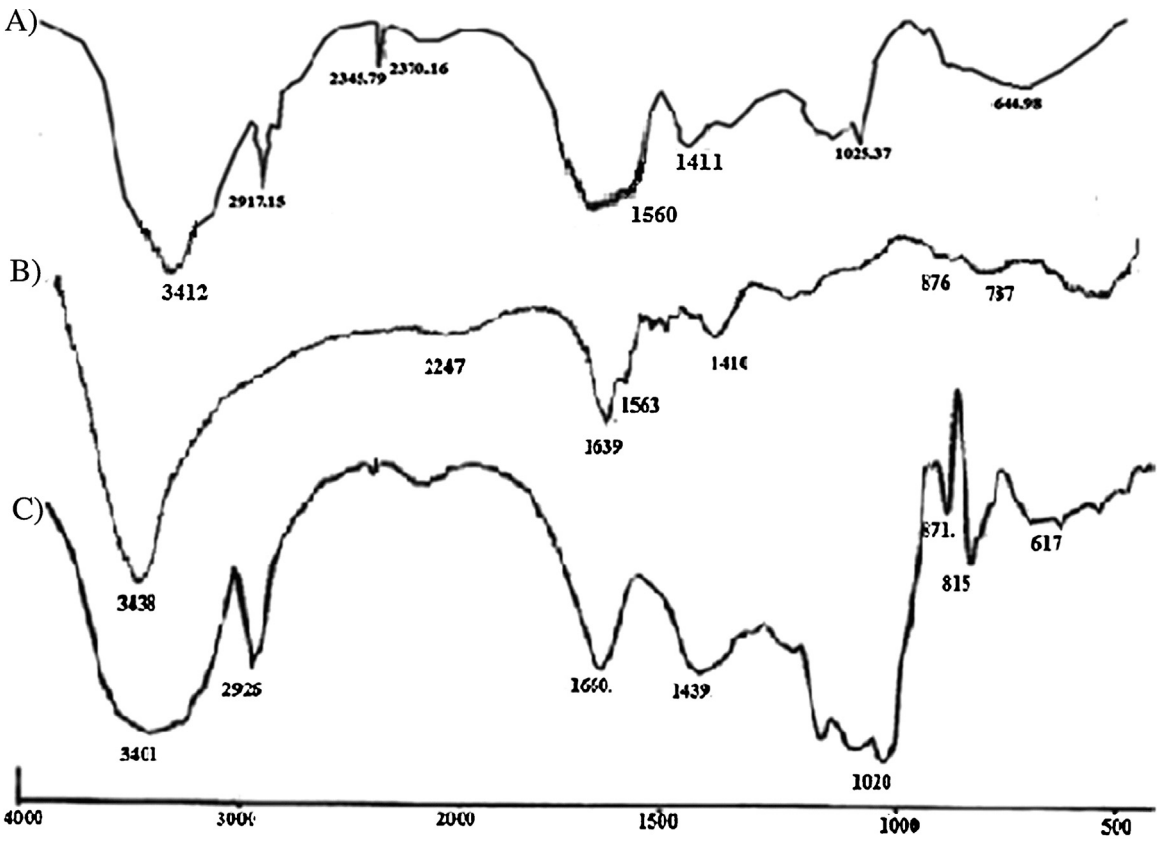

Fig 1. FT-IR spectra of (A) SPH, (B) Monomer and (C) Back bone.

Bands of GG at 1020 cm^{-1} (C—O stretching), 1082 (C—OH stretching) and 1158 cm^{-1} (C—O—C stretching), although are visible in the spectrum of hydrogel, the intensity is weaker. Shift of ≈30 cm^{-1} towards longer wavelength in the O—H stretching band in hydrogel can be attributed to inter/intramolecular H—bonding. Absence of all the characteristic peaks of $CONH_2$ group of acrylamide and appearance of characteristic of peaks of —COOH group confirm hydrolysis of amide to —COOH group. During synthesis of SPH, it was observed that after addition of $NaHCO_3$ and onset of polymerisation, pH of the medium increased to pH 12. This may explain the conversion of $-CONH_2$ to —COOH and $-COO^-$ groups, accompanied by evolution of NH_3.

3.1.2. Solid state C^{13} NMR analysis

Fig. 2 depicts ^{13}C NMR spectrum of an optimized crosslinked porous hydrogel. NMR peaks in the spectrum were compared with the peaks of native GG. A signal at 181.5 ppm can be ascribed to the COO^- group of Cs in the grafted PA network. This peak is not visible in the spectrum of GG. Assignments characteristic of the GG are clearly visible in the spectrum of the hydrogel and are as follows (Kriz, Dybal, & Dautzenberg, 2001): 103.6 ppm (C_1 of galactose and mannose units), 101.9 ppm (C_1 of b-D-mannose-reducing chain end), 72.5 ppm (C_2–C_5 of galactose and mannose), and 64 ppm broad peak (C_6 of galactose and mannose units). Additional peaks at 39.03–43.33 ppm can be assigned to various Cs (CH_2—CH_2—) of the polyacrylate network grafted onto the GG. The absence of peaks in this region in the backbone's spectrum confirms *in situ* grafting and crosslinking.

3.1.3. Scanning electron microscopy analysis

Morphology of a representative SPH examined by SEM at various magnifications is given in Fig. 3. It is clearly visible from the images that the SPH contains large number of pores of different sizes. Dried hydrogel contains large number of pores of different sizes. Pore size was estimated from the images by averaging the diameter of ten cells. The average pore diameter calculated as 5.87 μm. The images show that presence of guar gum and its participation in the polymerisation did not destroy or affect the porous morphology of SPH. SEM photograph of GG displays dense and smooth surface of the backbone is shown in Fig. 3. As is evident from Fig. 3, grafting and crosslinking of PA chains onto the backbone resulted in homogeneous but fractured topography which appears nonporous in topography. In SEM of SPH, the opaque surface surrounding the pores is assigned to the polysaccharide guar gum which is very conspicuous due to high biopolymer-monomer ratios employed in the present study.

Table 3
Elemental composition of prepared guar gum based superporous hydrogels.

Sample	Nitrogen (%)	Carbon (%)	Hydrogen (%)
Guar gum	0.639	38.55	7.571
SPH-1 (0.3% AM)	7.829	39.71	7.644
SPH-2 (0.5% AM)	11.67	41.79	7.649
SPH-3 (0.7% AM)	11.78	45.80	7.646

3.1.4. Elemental analysis

As compared to the backbone, higher content of C, H and N in SPHs indicates grafting of polyacrylamide/polyacrylate chains on to the backbone. The data in presented in Table 3. Increase in the percent grafting with increase in monomer concentration is evident as the percent C and N follows the order SPH-3 > SPH-2 > SPH-1.

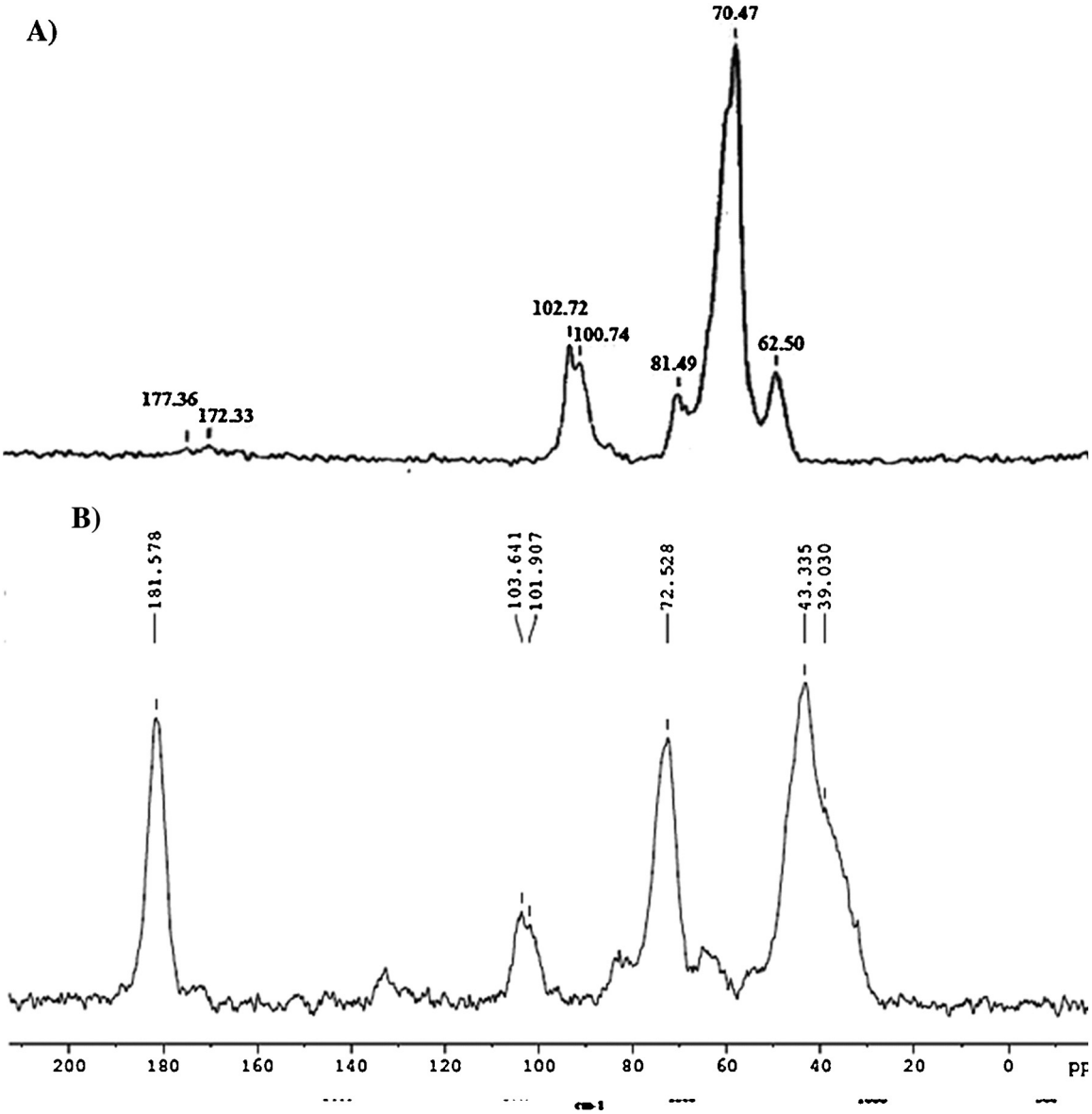

Fig. 2. ^{13}C NMR spectra of guar gum (A) and SPH (B) (solid-state ^{13}C).

3.2. SPH polymer synthesis and effect of sequence of addition of reactants and reaction variables on water absorbency behaviour

Major reactions steps involved in the preparation of SPHs are gelation and foaming. In order to generate uniform pores in the matrix of the hydrogel, harmonization between foaming and gelation is the key element. As described by Omidian, Roccaa, and Park (2005); the whole process can be divided into three stages. Stage I involves pre-gelation foaming, characterized by non-significant rise in temperature. In Stage II, the foaming process gets over and is characterized by about 8 °C increase in temperature of feed mass. In Stage III, the fluid foaming mass transforms into solid flexible rubbery form and temperature attains its peak (80 °C). Stage-II involving synchronized gel and pore formation is most critical. A general synthetic procedure reported in most of the studies (Omidian et al., 2005) was followed with little modification. Sequence of addition of various reactants may play some role in the preparation of SPHs, an aspect which has not been investigated systematically in the reported literature.

In the present study, six methods differing in the sequence of addition of various reagents and reaction conditions were investigated (Table 2). The effect of different methods on water absorbency of the prepared SPHs is shown in Fig. 4. As is clear from Fig. 4, SPHs from methods-II, III and V exhibited statistically similar and superior absorbency in distilled water as compared to I, IV and VI. It was observed that the hydrogels prepared by different methods exhibited statistically similar water absorbency, product from method II had slightly higher water absorbency (40 g/g) compared to other methods. This implies that sequence of addition of reactants does not influence the swelling characteristics of porous hydrogels, although the addition of foam stabilizer before onset of gelling is more favoured.

Cross linker plays an important role in influencing the SPH properties (Kabiri, Omidian, Hashemi, & Zohuriaan-Mehr, 2003). Effect of cross linker content on the water absorbency of SPHs is shown in Table 4. As can be seen from Eq. 1, foaming aid reacts with sodium bicarbonate, carbon dioxide gas bubbles start evolving. Efficiency of the trapping the gas bubbles during gelation determines the porosity of SPH. Increase in cross linker concentration favours high rate

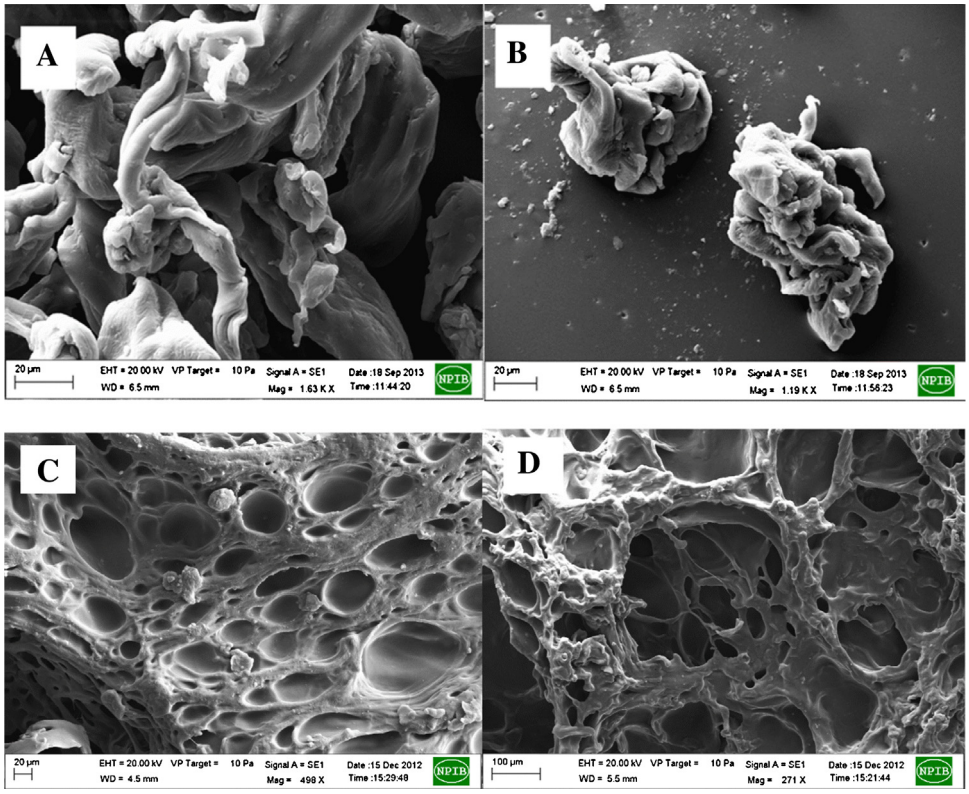

Fig. 3. SEM images of guar gum (A and B) and SPH (C and D).

$$R - COOH + NaHCO_3 \rightarrow R - COONa + CO_2 \uparrow + H_2O$$

Eq. 1. Scheme of reaction between foaming aid and sodium bicarbonate (SBC).

Table 4
Effect of various synthesis parameters on water absorbency of prepared hydrogels.

Cross linker concentration[a] (wt%)	Water absorption Q_{H_2O} (g/g)	Foam stabilizer concentration[b] (wt%)	Water absorption Q_{H_2O} (g/g)	Water volume[c] (ml/g)	Water absorption Q_{H_2O} (g/g)	Porogen concentration[d] (wt%)	Water absorption Q_{H_2O} (g/g)
0.01	11.2^{c}	0.0	22.7^{e}	1.98	26.3^{e}	0.1–0.5	32.9^{g}
0.03	16.8^{bc}	0.3	25.6^{d}	3.96	37.8^{c}	00.7–1.2	48.3^{a}
0.1	20.3^{b}	1.8	35.9^{c}	5.95	48.3^{a}	1.4–2.2	46.36^{b}
0.3	45.3^{a}	3.6	43.5^{a}	7.93	39.7^{b}	2.3–2.9	44.9^{c}
0.7	47.2^{a}	7.3	40.6^{b}	9.92	33.1^{d}	3.1–4.4	40.9^{d}
						4.8–6.6	38.2^{e}
						6.9–9.1	35^{f}
LSD at 5%	6.18		1.20		1.47		0.91
CV	11.65		1.89		2.11		1.25
F value	79.01		617.94		325.13		393.39

Mean values of Q_{H_2O} within a column followed by different letters in the superscript are significantly different at 5% level of significance and those followed by the same letter do not differ significantly at 5% level of significance.

[a] Synthesis parameters: weight ratio of monomer, initiator, foam stabilizer, porogen to backbone: 1.5:1, 0.05:1, 0.1:1 and 0.1:1, respectively, V_{H_2O} 5.95 ml/g feed.
[b] Synthesis parameters: weight ratio of monomer, cross linker, initiator, porogen to backbone: 1.5:1, 0.01:1, 0.05:1 and 0.1:1, respectively, V_{H_2O} 5.95 ml/g feed.
[c] Synthesis parameters: weight ratio of monomer, cross linker, initiator, foam stabilizer, porogen to backbone: 1.5:1, 0.01:1, 0.05:1, 0.1:1 and 0.1:1, respectively.
[d] Synthesis parameters: weight ratio of monomer, cross linker, initiator and foam stabilizer to backbone: 1.5:1, 0.01:1, 0.05:1 and 0.1:1, respectively, V_{H_2O} 5.95 ml/g feed.

of gelation. The increasing viscosity inhibits the CO_2 bubbles to escape from the gel mass and generates porous structure, which are manifested in the enhanced water absorbency. Similar observation has been reported by Kabiri et al. (2003). In the present study, at cross linker concentration >0.735 wt%, extensive rise in cross linking restricts the macromolecular relaxation and the consequent rise in swelling. The schematic representation of grafting and crosslinking of polymer chains onto guar gum is depicted in Fig. 5.

Fig. 6 shows that FS-4 behaves as the best foam stabilizer. Performance of a foam stabilizer is determined by the length of duration up to which the foam is sustained (Chen & Park, 2000). Effect of the concentration of the optimized foam stabilizer on water absorbency is presented in Table 4. It is clear from the table that increase in the concentration of foam stabilizer from 0.00 to 7.35 wt.% led to significant increment in the Q_{H_2O} values of the corresponding SPHs.

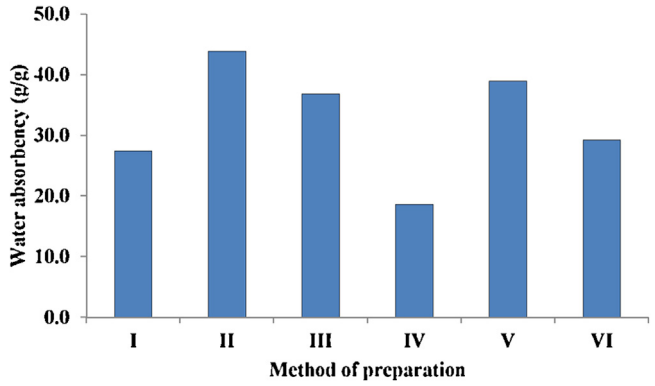

Fig. 4. Effect of method of preparation on water absorbency of SPH.
LSD at 5% degrees of freedom is 5.22, CV is 8.8 and F value between treatments is 30.44. Synthesis parameters: weight ratio of monomer, cross linker, initiator, foam stabilizer, porogen to backbone: 1.5:1, 0.01:1, 0.05:1, 0.1:1 and 0.1:1, respectively, V_{H_2O} 5.95 ml/g feed.

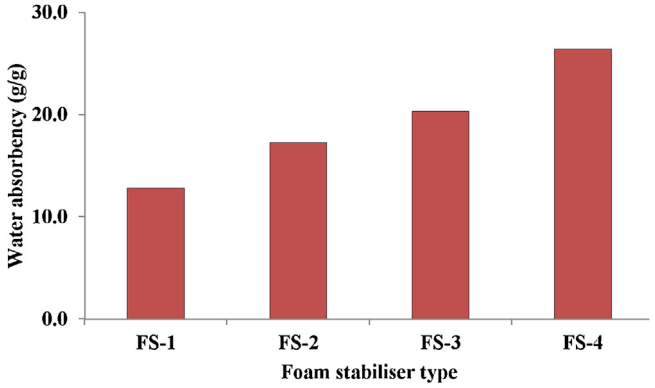

Fig. 6. Effect of foam stabilizer type on water absorbency of SPH.
LSD at 5% degrees of freedom 1.24, CV is 3.246 and F value between is 250.45. Synthesis parameters: weight ratio of monomer, cross linker, initiator, foam stabilizer, porogen to backbone: 1.5:1, 0.01:1, 0.05:1, 0.1:1 and 0.1:1, respectively, V_{H_2O} 5.95 ml/g feed.

Concentration of the porogen influences the swelling properties of the hydrogels. As is clear from Table 4, porogen concentration in the range of 0.07–1.2%, resulted in the SPHs with maximum WAC. At higher concentrations, consistently low swelling behaviour was exhibited by the SPHs. Under acidic pH conditions employed (pH 5–5.5), SBC reacts with acid to generate CO_2 gas bubbles. Beyond an optimum concentration of the porogen, the pH of the reaction medium tends to rise which adversely affects the gelation process. This effect is reflected in inferior water absorbency values of the resulting SPH. Similar observation on the performance of pH-sensitive SPHs has been reported earlier (Chen, Blevins, Park, & Park, 2000).

As is evident, water serves as the medium for gelation and foaming processes to occur smoothly. Its quantity per unit feed mass was studied as a variable against the swelling capacity Q_{H_2O} of the prepared SPH. The results presented in Table 4, indicated the significant increase in Q_{H_2O} with increase in water volume up to 5.95 ml/g feed. On further increase gelation failed to occur and SPHs were not formed. An optimum dilution leads to effective collisions of the monomer and cross linker free radicals with the grafting sites of the back bone, leading to increase in gelation rate and effective entrapment of gas bubbles in the expanding gel. At higher dilutions, namely low monomer concentration and availability of more molecular oxygen in the reaction mixture play adverse role and the gel fails to form.

In previous reports on SPHs (Kuang, Yuk, & Huh, 2011; Chen & Park, 2000; Chavda & Patel, 2010), acetic acid or acrylic acid were most commonly employed foaming aids. In our efforts to find better alternative to these toxic reagents, three organic acids were evaluated for their pore inducing ability. The results are shown in Fig. 7. SPH prepared by using oxalic acid (OA-3), exhibited most superior water absorbency value, as compared to acetic acid (OA-1) and citric acid (OA-2). Release of higher number of moles of CO_2 in the presence of OA-3 as compared to OA-1 and OA-2 at a particular concentration of sodium bicarbonate (SBC) may explain the observed behaviour. A comparison with hydrogel prepared in the absence of the foaming aid (Q_{H_2O} 22.7 g/g) justifies the role of foaming aid in influencing the swelling characteristics of hydrogels.

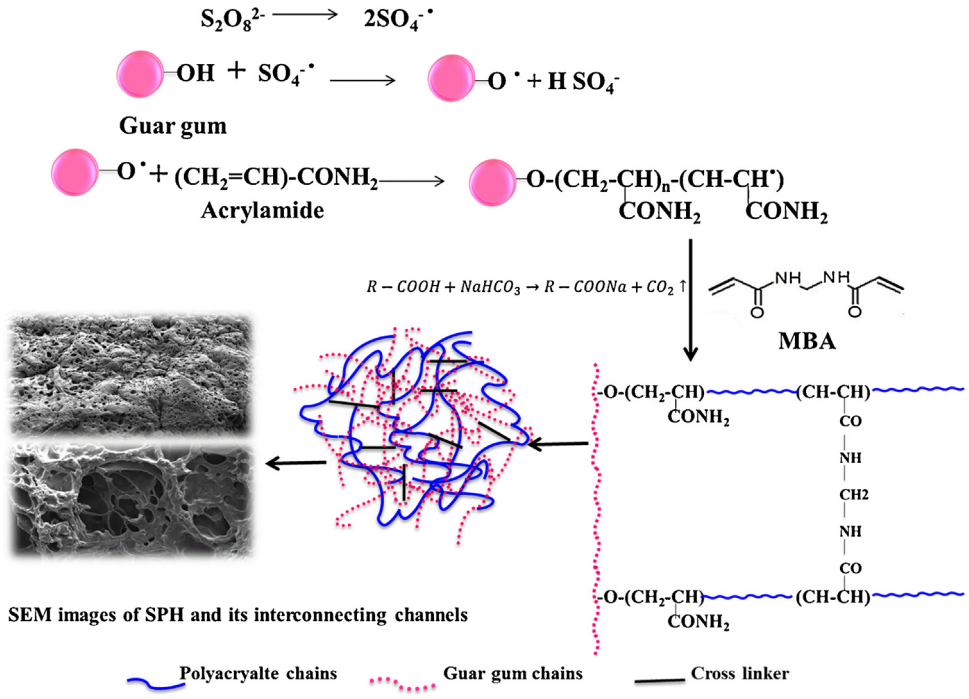

Fig. 5. Diagrammatic representation of formation of a typical cross linked guar gum based super porous hydrogel.

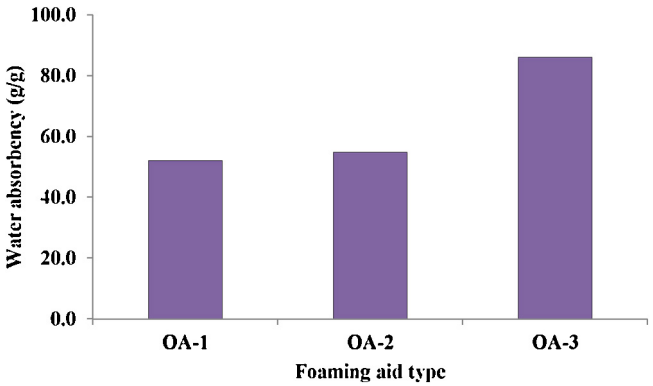

Fig. 7. Effect of foaming aid type on water absorbency of SPH.
LSD at 5% degrees of freedom is 1.90, CV is 1.30 and F value between treatments is 1524.13, synthesis parameters: weight ratio of monomer, cross linker, initiator, foam stabilizer, porogen to backbone: 1.5:1, 0.01:1, 0.05:1, 0.1:1 and 0.1:1, respectively, V_{H_2O} 5.95 ml/g feed.

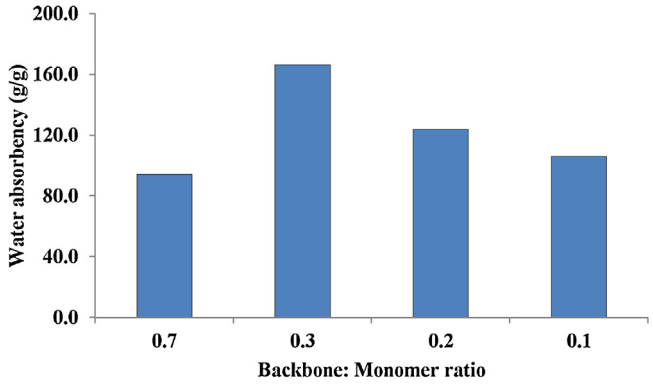

Fig. 8. Effect of backbone: monomer ratio on water absorbency of SPH.
LSD at 5% degrees of freedom 1.19, CV is 1.53 and F value between 975.31. Synthesis parameters: weight ratio of monomer, cross linker, initiator, foam stabilizer and porogen tobackbone:1.5:1, 0.01:1, 0.05:1, 0.1:1 and 0.1:1, respectively, V_{H_2O} 5.95 ml/g feed.

In biopolymer based porous hydrogels, backbone-monomer ratio significantly influences the swelling properties of the finished product. In most of the studies reported so far (Chen & Park, 2003; Yin et al., 2007) the backbone-monomer ratio was kept very low (<0.2). Synthesis in these studies was intended to generate extremely fast swelling porous hydrogels for their use as gastric retention release devices, where fast delivery of the inputs is desirable. In the present study, carrier properties of porous hydrogels to entrap agriculturally important microbes are of interest. Stability requirements over a range of temperatures coupled with biocompatibility of carrier with the microbes necessitated presence of higher biopolymer content in the finished products. The effect of backbone-monomer ratio on the swelling characteristic of the SPHs is presented in Fig. 8. It is clear from the figure that higher backbone content in the feed decreased the swelling potential of the product. This can be ascribed to the fact that higher concentration of polysaccharide leads to the increase in the viscosity of reaction medium and also restricts the disentanglement of polymer chains.

3.3. Effect of duration of reaction on water absorbency

The gelation and foaming processes in the hydrogels prepared in present study were achieved in less than 2 min. However, in order to obtain a stable network, the graft polymerization reaction was allowed to continue for different time periods.

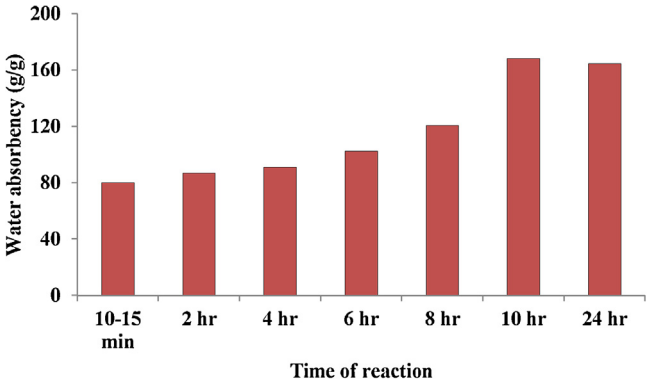

Fig. 9. Effect of duration of reaction on water absorbency of SPH.
LSD at 5% degrees of freedom 1.19, CV is 1.53 and F value between 975.31. Synthesis parameters: weight ratio of monomer, cross linker, initiator, foam stabilizer and porogen to backbone: 1.5:1, 0.01:1, 0.05:1, 0.1:1 and 0.1:1, respectively, V_{H_2O} 5.95 ml/g feed.

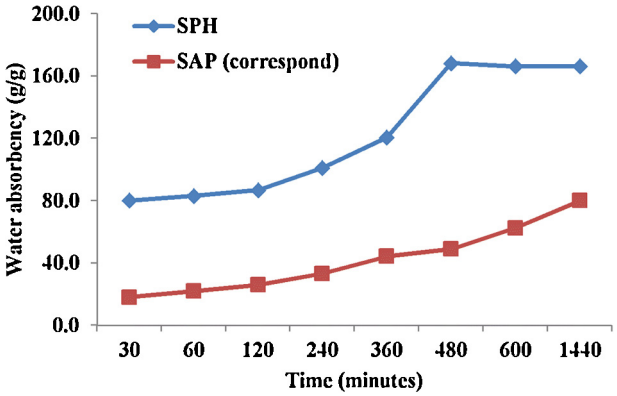

Fig. 10. Effect of time period on water absorbency of SPH vs. GG-SAP.
LSD at 5% degree of freedom iss 4.33, CV is 4.09 and F value is 1436.1

SPHs generated were evaluated for their swelling behaviour in distilled water. The results are shown in Fig. 9. The 6 h reaction yielded SPH with highest Q_{H_2O} (52.3 g/g). Reaction time more than 6 h resulted in decrease in water absorbency. This can be attributed to increase in the cross-link density and screening of pores by the polymer network chains, when polymerization is allowed after an optimum time period.

3.4. Swelling rate

Comparative variation of Q_{H_2O} of SPH vs. corresponding porogen free SAP with time in distilled water at 50 °C is shown in Fig. 10. It is evident the SPH swells fast attaining 50% absorbency in 30 min. After 30 min, swelling ratio consistently increased and attained its maximum equilibrium swelling in 6 h. The porogen free SAP, on the other hand reached its Q_{H_2O} maximum in 24 h. Initial fast swelling in case of SPH is due to capillary action through fast action through the pores. Later on, macromolecular expansion seems to influence the swelling rate. In case of SAP, the swelling occurs at much slower rate and is diffusion controlled.

3.5. Effect of external environment on water absorbency

The effect of temperature of the swelling medium *i.e.*, on the water absorbency of SPH is shown in Fig. 11. Rise in temperature of swelling medium exhibited increase in Q_{H_2O}. Maximum swelling is observed at 50 °C. This behaviour can be due to the extensive

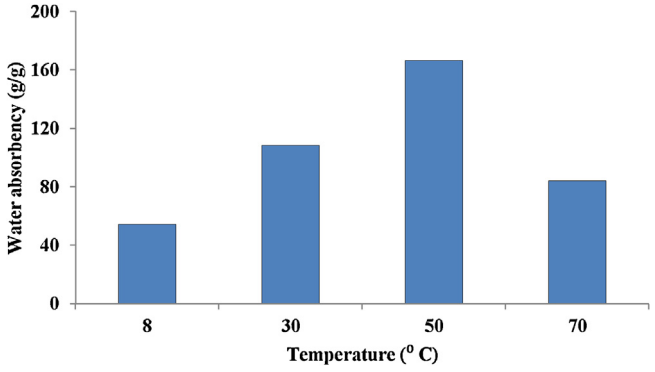

Fig. 11. Effect of temperature of swelling medium on water absorbency of SPH.

entanglement or expansion of the macromolecular chains at higher temperatures.

The swelling behaviour of SPH in different pH environments is presented in Table 5. At pH 9, the hydrogel shows maximum swelling. This can be explained in terms of ionization of the amide and –COOH groups to COO^- groups. The electrostatic repulsion between the COO^- groups leads to macromolecular expansion and the resulting enhancement of Q_{H_2O}. In acidic pH, protonation of the $-CONH_2$ and $-COO^-$ groups leads to decrease in extent of hydrogen bonding with water molecules and thus the decrease in water absorbency. Similarly findings have been confirmed in previous studies on SPHs and SAPs (Singh et al., 2010).

Swelling behaviour of the SPH in different salt solutions namely ammonium sulphate (AS), ammonium nitrate (AN), potassium nitrate (PN), sodium chloride (SC) and fertilizer urea solution, of strengths 5 mM, 10 mM, 15 mM and 20 mM is depicted in Table 6. It is clear from Table 6, that the hydrogel shows drastic reduction in its swelling tendency in all the salt solutions. Similar observation has been reported by Gils, Ray, and Sahoo (2009). The cations in the salt solutions screen the polar groups causing reduction in the hydrogen bonding with H_2O molecules. Also, in the salt solutions, the osmotic pressure resulting from the difference in mobile ion concentration between the gel matrix and the surrounding aqueous phase decreases, adversely affecting absorbency. In urea solution also, the absorbency exhibited fall with increase in its concentration from 5 mM to 20 mM, though the overall reduction in Q_{H_2O} was lesser than that in salt solutions.

In our previous work (Singh et al., 2010) we have reported that water quality also influences the swelling performance of hydrogels. The effect of water quality on the swelling behaviour of SPH is shown in Table 5. As compared to deionized water, absorbency is significantly reduced in different aqueous environments. The observed behaviour may be attributed to the reduction in osmotic potential between gel and the surrounding water containing cations of varying strengths (Pourjavadi, Seidi, Salimi, & Soleyman, 2008).

Table 7
Effect of cross linker concentration on density and porosity of prepared hydrogels.

Cross linker concentration (g)	Density (g/cc)	Porosity (%)
0.0005	0.61^e	79.9^a
0.001	0.67^d	70.7^b
0.005	0.71^c	63.2^c
0.01	0.79^b	58.4^d
0.02	0.86^a	32.8^e
LSD at 5%	0.012	2.20
CV	0.92	1.92
F value	603.39	686.95

Mean values of Q_{H_2O} within a column followed by different letters in the superscript are significantly different at 5% level of significance ($p < 0.0001$) and those followed by the same letter in the superscript do not differ significantly at 5% level of significance.

3.6. Porosity and density measurements

Effect of variation in cross linker concentration on the density and porosity of the *cl*-guar gum-*g*-poly(acrylate) SPHs is presented in Table 7. The results shown here offer an interesting pattern in contrast to previous studies reported on SPHs. Density of the SPHs increased with the increase in cross linker concentration whereas porosity varied inversely. Conventionally as described by Kabiri et al. (2003), higher cross linker concentrations should lead to shorter gelation times due to which the CO_2 gas bubbles cannot escape from the reaction mixture and thus the porosity increases. Similarly, due to generation of high foam volume, density of the hydrogel decreased with increase in cross linker concentration. The ironical findings in the present study can be understood as follows. For the network formation of optimum crosslinking density, a threshold quantity of cross linker is necessary which is specific to the experimental conditions, back bone nature and content *etc*. The minimum cross linker concentration screened in the present study was in the range of 0.005–0.02 wt% and the maximum was 0.7–0.8 wt%. The screened concentration range is much lower than that reported previously (Chavda & Patel, 2010; Kabiri et al., 2003). Low crosslinker content may not be just sufficient to generate a network through grafting and cross linking. Therefore an increase in the density and decrease in porosity is observed with increase in concentration of the cross linker. Findings from the present study will be utilised in our future endeavours, to develop cost effective process for production of guar gum based porous hydrogels.

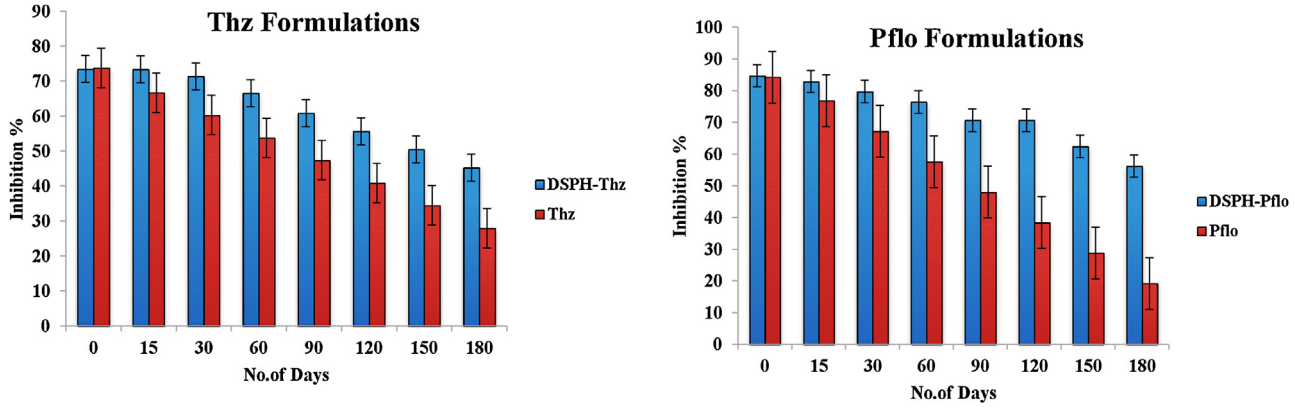

Fig. 12. Bioefficacy of formulations and control stored at 25 °C. (DSPH-*Thz*)-Dry formulation of *Thz* in SPH, (DSPH-*Pflo*)-Dry formulation of *Pflo* in SPH

Table 5
Effect of pH and quality of water on water absorbency of GG-SPH.

pH of water	Water absorption Q_{H_2O} (g/g)	Quality of water	Water absorption Q_{H_2O} (g/g)
Acid (4)	43.1[c]	Deionized water	196.8[a]
Neutral (7)	164.5[b]	Distilled water	166.2[b]
Alkaline (9)	199.6[a]	Tap water	114.6[c]
		Hard water –A	85.9[d]
		Hard water –B	61.8[e]
		Hard water –C	38.7[f]
LSD at 5%	4.44		5.40
CV	1.44		2.68
F value	5250.30		1270.81

Mean Q_{H_2O} values within a column followed by different letters in the superscript are significantly different at 5% level of significance and those followed by the same letter do not differ significantly at 5% level of significance.

Table 6
Effect of salt/fertilizer type and their strength on water absorbency of GG-SPH.

	Water absorption at different salt concentration (Q_{H_2O} (g/g))			
Salt/Fertilizer type	5 mM	10 mM	15 mM	20 mM
$(NH_4)SO_4$	51.83[h]	34.5[kl]	21.4[mn]	19.2[n]
NH_4NO_3	62.6[g]	42.8[j]	40.6[j]	32.5[l]
KNO_3	68.5[f]	51.8[h]	45.9[i]	40.9[j]
NaCl	71.6[e]	51.4[h]	36.2[k]	23.2[m]
NH_2CONH_2	133.4[a]	110.6[b]	94.1[c]	76.7[d]
LSD at 5%	2.41			
CV	2.62			
F value	1269.57			

Mean values of Q_{H_2O} within a table followed by different letters in the superscript are significantly different at 5% level of significance and those followed by the same letter do not differ significantly at 5% level of significance.

Table 8
Shelf life of bioagents in formulations and control at 25 °C storage temperature (Log CFUs).

Formulation	DAYS									
	0	15	30	60	90	120	150	180	LSD	SD
DSPH-*Thz*	11.0[a]	10.8[ab]	10.7[bc]	10.7[c]	10.4[d]	10.2[e]	10.1[e]	9.8[f]	0.129	0.40
DSPH-*Pflo*	11.0[a]	11.0[a]	10.9[b]	10.9[b]	10.8[c]	10.6[d]	10.2[e]	9.9[f]	0.086	0.39
Thz	11.0[a]	10.0[b]	8.0[c]	6.5[d]	4.7[e]	2.2[f]	0.9[g]	0.5[h]	0.122	4.06
Pflo	11.1[a]	10.1[b]	8.1[c]	6.6[d]	4.8[e]	2.3[f]	1.0[g]	0.6[h]	0.034	4.06

Mean values of Log CFUs within a row followed by different letters in the superscript are significantly different at 5% level of significance ($p < 0.0001$) and those followed by the same letter in the superscript do not differ significantly at 5% level of significance.
(DSPH-*Thz*)-Dry formulation of *Thz* in SPH, (DSPH-*Pflo*)-Dry formulation of *Pflo* in SPH.

3.7. *Shelf life and bioefficacy (*in vitro*) evaluation of SPH microbial formulations*

Shelf life of formulations *vis-à-vis* controls evaluated periodically is presented in Table 8. It is evident that SPH hydrogel played a significantly favourable role in providing moisture rich environment and retaining the viability of immobilized microbes for prolonged duration as compared to control. The results are in line with the similar work reported earlier on entomopathogenic nematodes immobilized in wet gel formulations (Ganguly, Anupama, Kumar, & Parmar, 2008).

Bioefficacy *(in vitro)* appraisal of prepared compositions *vis-à-vis* control against pathogen (*P. aphanidermatum*) is shown in Fig. 12. The results clearly indicate the significantly superior performance of hydrogel based fungal and bacterial formulations over control that carrier potential in release of microbes in a controlled manner. In a similar study, Mondal and Anupama (2012) showed the improved bioefficacy of *Trichoderma* sps. mycelia based hydrogel formulations against *Rhizoctonia solani*.

4. Conclusions

Novel series of guar gum-*g*-poly(acrylate) porous superabsorbent hydrogels (SPH) were prepared employing free radicle initiated open air grafting polymerization technique. Effect of reaction parameters and reagents on the swelling behaviour of SPHs was investigated. Variation of concentration of the cross linker led to *hitherto unreported* observations regarding its effect on the swelling behaviour, porosity and density of dry SPH. SEM analysis of the hydrogel revealed porous structure. This feature coupled with the biocompatible character of guar gum backbone indicates potential of these SPHs as carriers of agro-inputs such as agriculturally important microbes, pesticides and fertilizers. Shelf life and bioefficacy data of biocontrol fungus and bacteria immobilized in a prepared SPH established the porous hydrogel's potential as an effective carrier. In our future endeavour, the SPH will be further explored as carrier materials to entrap microbes and herbicides together coupled with optimized swelling characteristics.

Acknowledgements

Authors are thankful to ICAR-Indian Agricultural Research Institute, New Delhi and Post Graduate School of the Institute for providing funds to conduct this research.

References

Chavda, H., & Patel, C. (2010). Chitosan super porous hydrogel composite-based floating drug delivery system: a newer formulation approach. *Journal of Pharmacology and Biological Science*, *2*(2), 124–131.

Chavda, H. V., & Patel, C. N. (2009). Effects of solvent treatments on characteristics of super porous hydrogels. *Ethiopian Pharmacological Journal*, *27*, 16–24.

Chen, J., Blevins, W. E., Park, H., & Park, K. (2000). Gastric retention properties of super porous hydrogel composites. *Journal of Controlled Release*, *64*, 39–51.

Chen, J., Park, H., & Park, K. (1999). Synthesis of super porous hydrogels: hydrogels with fast swelling and superabsorbent properties. *Journal of Biomedical Material Research*, *44*, 53–62.

Chen, J., & Park, K. (2000). Synthesis and characterization of super porous hydrogel composites. *Journal of Controlled Release*, *65*, 73–82.

Chen, X. G., & Park, H. J. (2003). Chemical characteristics of *O*-carboxymethylchitosans related to its preparation conditions. *Carbohydrate Polymers*, *53*, 355–359.

Choi, Y. M., Im, S. J., Myung, S. W., Choi, H. S., Park, K., & Huh, K. M. (2007). Preparation and swelling behaviour of super porous hydrogels: control of pore structure and surface property. *Key Engineering Materials*, *342*, 717–720.

Daasch, L. W. (1947). Infrared spectroscopic analysis of five isomers of 1,2,3,4,5,6-hexachlorocyclohexane. *Analytical Chemistry*, *19*, 779–785.

Ganguly, S., Anupama, Kumar, A., & Parmar, B. S. (2008). Nemagel—a formulation of the entomopathogenic nematode *Steinernema thermophilum* mitigating the shelf-life constraint of the tropics. *Nematologia Mediterrania*, *36*(2), 125–130.

Gils, P. S., Ray, D., & Sahooa, P. K. (2009). Characteristics of xanthan gum-based biodegradable super porous hydrogel. *International Journal of Biological Macromolecules*, *45*, 364–371.

Guo, B. L., & Gao, Q. Y. (2007). Preparation and properties of a pH/temperature responsive carboxymethyl chitosan/poly(*N*-isopropylacrylamide) semi-IPN hydrogel for oral delivery of drugs. *Carbohydrate Research*, *342*, 2416–2422.

Guo, J. H., Skinner, G. W., Harcum, W. W., & Barnum, P. E. (1998). Pharmaceutical applications of naturally occurring water-soluble polymers. *Pharmaceutical Science & Technology Today*, *1*, 254–261.

Hyojin, P., Kinam, P., & Dukjoon, K. (2006). Preparation and swelling behavior of chitosan-based super porous hydrogels for gastric retention application. *Journal of Biomedical Material Research*, *76*, 144–150.

Kabiri, K., Omidian, H., Hashemi, S., & Zohuriaan-Mehr, M. J. (2003). Synthesis of fast swelling superabsorbent hydrogels: effect of crosslinker type and concentration on porosity and absorption rate. *Environmental Protection Journal*, *39*, 1341–1348.

Kasgoz, H., & Durmus, A. (2008). Dye removal by a novel hydrogel-clay nanocomposite with enhanced swelling properties. *Polymers for Advanced Technologies*, *19*, 838–845.

Kim, D., & Park, K. (2004). Swelling and mechanical properties of super porous hydrogels of poly(acrylamide-*co*-acrylic acid)/polyethylenimine interpenetrating polymer networks. *Polymer*, *45*, 189–196.

Kosemund, K., Schlatter, H., Ochsenhirt, J. L., Krause, E. L., Marsman, D. S., & Erasala, G. N. (2009). Safety evaluation of superabsorbent baby diapers. *Regulatory Toxicology and Pharmacology*, *53*, 81–89.

Kriz, J., Dybal, J. A., & Dautzenberg, H. (2001). Cooperative interactions of unlike macromolecules: NMR and theoretical study of the electrostatic coupling of sodium polyphosphates with diallyl-(dimethyl) ammonium chloride-acrylamide copolymers. *Journal of Physical Chemistry*, *105*(31), 7486–7493.

Kuang, J., Yuk, K. Y., & Huh, K. M. (2011). Polysaccharide-based super porous hydrogels with fast swelling and superabsorbent properties. *Carbohydrate Polymers*, *83*, 284–290.

Omidian, H., & Park, K. (2002). Experimental design for the synthesis of polyacrylamide super porous hydrogels. *Journal of Bioactive and Compatible Polymer*, *17*, 433–450.

Omidian, H., Rocca, J. G., & Park, K. (2006). Elastic: super porous hydrogel hybrids of polyacrylamide and sodium alginate. *Macromolecular Bioscience*, *6*, 703–710.

Omidian, H., Roccaa, J. G., & Park, K. (2005). Advances in super porous hydrogels. *Journal of Control Release*, *102*, 3–12.

Park, K., Shalaby, S. W. S., & Park, H. (1993). Biodegradable hydrogels for drug delivery. *Journal of Applied Polymer Science*, *74*, 119–124.

Pourjavadi, A., Seidi, F., Salimi, H., & Soleyman, R. (2008). Grafted CMC/silica gel superabsorbent composite: synthesis and investigation of swelling behaviour in various media. *Journal of Applied Polymer Science*, *108*, 3281–3290.

Puoci, F., Iemma, F., & Spizzirri, U. G. (2008). Polymers in agriculture: a review. *American Journal of Agricultural and Biological Sciences*, *3*, 299–314.

Prithusayak Mondal and Anupama (2012). Integrated formulation of neem oil, Trichoderma harzianum and zinc for management of sheath blight and zinc in rice. A M.Sc. thesis submitted to Indian Agricultural Research Institute.

Singh, A., Sarkar, D. J., Singh, A. K., Prasad, R., Kumar, A., & Parma, B. S. (2010). Studies on novel nano-superabsorbent composites: swelling behaviour in different environments and effect on water absorption and retention properties of sandy loam soil and soil-less medium. *Journal of Applied Polymer Science*, *120*, 1448–1458.

Sinha, V. R., & Kumria, R. (2001). Polysaccharides in colon-specific drug delivery. *International Journal of Pharmaceutics*, *224*, 19–38.

Tang, C., Yin, C. H., Pei, Y. Y., Zhang, M., & Wu, L. F. (2005). New super porous hydrogels composites based on aqueous carbopols solution (SPHCs): synthesis, characterisation and in vitro bioadhesive force studies. *European Polymer Journal*, *41*, 557–562.

Wang, Q., Zhang, J., & Wang, A. (2009). Preparation and characterization of a novel pH-sensitive chitosan-*g*-poly(acrylic acid)/attapulgite/sodium alginate composite hydrogel bead for controlled release of diclofenac sodium. *Carbohydrate Polymers*, *78*, 731–737.

Yin, L., Fei, L., Cui, F., Tang, C., & Yin, C. (2007). Superporous hydrogels containing poly(acrylic acid-*co*-acrylamide)/*O*-carboxymethyl chitosan interpenetrating polymer networks. *Biomaterials*, *28*, 1258–1266.

Zhang, J. P., Li, A., & Wang, A. Q. (2006). Study on superabsorbent composite: preparation: characterization and swelling behaviours of starch phosphate-graft-acrylamide/attapulgite superabsorbent composite. *Carbohydrate Polymers*, *65*, 150–158.